

# Wavelength Separation of Plus and Minus Orders of Soft-X-ray–EUV Multilayer-Coated Gratings at Near-Normal Incidence

Leonid I. Goray<sup>\*a, b</sup> and John F. Seely<sup>c</sup>

<sup>\*a</sup>International Intellectual Group, Inc., P.O. Box 335, Penfield, NY 14526, USA;

<sup>b</sup>Institute for Analytical Instrumentation, Russian Academy of Science, Rizhsky Pr. 26, Saint-Petersburg 190103, Russia;

<sup>c</sup>Space Science Division, Naval Research Laboratory, Washington DC 20375, USA

## ABSTRACT

The validity of approximating the efficiency of a multilayer grating operating at close to normal incidence in the soft-X-ray–EUV range with a product of the relative grating efficiency by the reflectance of its multilayer coating has been studied by the rigorous integral method. The widely used approximated approach has until recently been considered accurate enough for analysis of short-wavelength normal-incidence multilayer-coated gratings. Real gratings employed in the soft-X-ray–EUV range are used to demonstrate the inapplicability of this approximation to an analysis of precise positions of efficiency maxima for the external ( $n > 0$ ) and internal ( $n < 0$ ) diffraction orders, despite the small ratios of wavelength and groove depth to period. The present authors have performed an analysis of the accuracy inherent in a derived simple expression for spectral separation of the same plus and minus orders with respect to the wavelength, order's number, incident angle, period, and groove depth. The reason for the observed substantial (a few Angstrom or even nm) wavelength separation between the maxima of positive and negative orders is related to oblique, close-to-normal incidence of radiation on a grating operating in the short-wavelength spectral region and different angles of deviation of respective orders. The modeling carried out with the commercial code PCGrate-S(X) v.6.1 permitted not only prediction of the separation between positive and negative orders for a multilayer Mo/Si 4200-gr/mm grating with AFM-measured trapezoidal groove profile, which is designed for operation in the EIS spectrometer on the Solar-B spacecraft, but obtaining a good agreement with synchrotron radiation measurements, including high orders as well. A conclusion is drawn that high-precision calculations of the efficiency of multilayer normal-incidence soft-X-ray–EUV range gratings have in some cases to be performed, although this may require increasing the computation time by several times compared to the commonly used approximate approach.

**Keywords:** diffraction grating, soft-X-ray–EUV spectroscopy, integral method, efficiency modeling, multilayer-coated X-ray optics

## 1. INTRODUCTION

A specific feature of gratings operating in the short-wavelength range is their small wavelength to period ratio. A grating is assumed to operate in scalar mode in order  $n$  if  $n\lambda/d < 0.2$ , and the angles of incidence,  $\theta$ , and diffraction,  $\theta'_n$ , are close to the grating normal. The scalar mode does not typically give rise to polarization effects or anomalies, and the efficiency of perfectly reflecting gratings is derived from universal curves constructed for different groove profiles<sup>1</sup>. Universal curves are functions of  $h/d$  only, and they are equally applicable to gratings with different periods, groove depth, and coating materials. To take into account finite conductivity of the grating material, one has only to multiply the value of efficiency extracted from the universal curve by the coating reflectance. Phenomenological approaches and the scalar theory of Fresnel–Kirchhoff<sup>2</sup> permit one quite frequently, despite the well-known limitations, to gain insight into a physical phenomenon and, thus, spare the costs of numerical modeling.

The desire to improve grating efficiency in the soft-X-ray–EUV range leads to the use of grazing angles of incidence and/or multilayer coatings, where scalar theory turns out invalid<sup>3,4</sup>. Gratings working in this range are characterized by a large number of propagating orders, as well as by a need of accounting for the effects of shadowing, absorption,

---

\*E-mail: [lig@pcgrate.com](mailto:lig@pcgrate.com); phone/fax: 585-218-9829; [www.pcgrate.com](http://www.pcgrate.com)

multiple reflections, multiwave scattering, polarization, and other nonscalar properties. While multilayer-coated diffraction gratings designed for operation near normal incidence in the soft-X-ray–EUV range hold the most promise, rigorous numerical modeling of their efficiency still remains fairly time consuming<sup>3</sup>. The most precise approach to an efficiency analysis of gratings with real, e.g., AFM-measured, groove profiles accounting for microroughness is the method of integral equations, which is applicable to systematic calculations in the short-wavelength range<sup>3-6</sup>.

The present communication considers the effect of spectral separation of positive and negative orders, which is inherent to various multilayer-coated short-wavelength gratings operating near normal incidence. Section 2 describes some aspects of scalar theory of diffraction on gratings and its limitations. Section 3 presents a phenomenological approach to the separation of the same plus and minus orders in wavelength discovered earlier. The approximate expression derived for the separation of orders is compared with the results obtained in rigorous numerical modeling of the efficiency of bulk, perfectly conductive lamellar gratings. A study of the efficiency of a multilayer-coated Mo/Si, 4200-gr/mm grating<sup>7</sup> with AFM-measured groove profile designed for the EIS spectrometer on Solar-B is described in Section 4. The measurements of absolute efficiency reformed in a synchrotron beam are compared with new calculations based on a rigorous multilayer modified integral method (MIM)<sup>8</sup>. All modeling results covered in this publication were obtained with a commercial program PCGrate-S(X) v.6.1<sup>9</sup>. Section 5 sums up the paper.

## 2. SOME ASPECTS OF SCALAR THEORY AND OF THE PERFECT CONDUCTIVITY APPROXIMATION

A calculation performed with the basis of the Kirchhoff approximation<sup>2</sup> yields for the maximum grating efficiency about 34, 40, and 100% for the sinusoidal, lamellar, and sawtooth groove profiles, respectively. These peaks exist always for a certain ratio of modulation (profile) depth to wavelength, which corresponds to a maximum of the universal curve in  $n$ th order autocollimation for  $\theta = \theta'_n$  (Littrow mounting):

$$2 \sin \theta = n\lambda_{\text{Lit}}/d. \quad (1)$$

For sawtooth profile gratings with a blaze angle  $\delta = \delta_B$  this maximum lies at

$$\lambda_{\text{Lit}}(n) = 2h_{\text{opt}}/n = 2d \sin \delta / n; \quad (2)$$

for lamellar gratings, at

$$\lambda_{\text{Lit}}(-1) = 4h_{\text{opt}}; \quad (3)$$

and for sinusoidal ones, at

$$\lambda_{\text{Lit}}(-1) \approx 3.4h_{\text{opt}}. \quad (4)$$

In addition to the very valuable asset of a high efficiency of gratings with triangular groove profile, scalar theory reveals another essential merit, namely, the lamellar profile provides the lowest efficiency in higher orders of the spectrum, a very important point if they have to be suppressed<sup>10</sup>. Gratings with an arbitrary (for instance, polygonal) groove profile are also characterized by an optimum depth, which corresponds to a maximum in the efficiency curve and is related to the coefficients of the groove profile expansion in a Fourier series.

The position of the maximum on the universal efficiency curve and its height vary smoothly as the grating operation deviates from the autocollimation mode. This variation is the smaller, the smaller the ratios  $n\lambda/d$  and  $h/d$ . As the deviation angle

$$D_n = \theta + \theta'_n \quad (5)$$

increases polarization effects appear, first for the Fresnel reflection coefficients of the coating materials, and subsequently, in the grazing angle range for perfectly reflecting gratings as well<sup>10</sup>. For other than grazing angles of incidence, an empirical expression relating the blaze wavelength to the similar autocollimation wavelength applies

$$\lambda_B = \lambda_{Lit} \cos(D_n/2). \quad (6)$$

The absolute efficiency of a soft-X-ray-EUV multilayer grating in the  $n$ th order,  $E_m^a(n)$ , was represented<sup>11</sup> by a product of the reflectance of a plane multilayer mirror in the  $m$ th Bragg order,  $R_m(\theta'')$ , by the efficiency of a perfectly reflecting grating  $E^p(n, \theta)$ :

$$E_m^a(n) = R_m(\theta'')E^p(n, \theta), \quad (7)$$

where  $\theta'' = \theta$  in a general case, and  $\theta'' = \theta - \delta$  for a sawtooth-profiled grating with a blaze angle  $\delta$  (the condition in which the incident ray and the diffraction order  $n$  are symmetric with respect to the working groove facet). For gratings operating in the grazing mode another approach was proposed<sup>3</sup>, which is based on the product of the reflectance of a multilayer mirror by the relative efficiency of a finitely conductive grating specified by one (substrate) corrugated boundary:

$$E_m^a(n) = R_m(\theta'')E_{Sub}^a(n, \theta)/R_{Sub}(\theta''). \quad (8)$$

In the case of a sawtooth profile, the rigorously calculated efficiency of a perfectly reflecting grating can be replaced by a phenomenological relation based on geometric considerations<sup>1</sup>:

$$E_m^a(n) = R_m(\theta - \delta) \min [\cos(\theta - 2\delta)/\cos \theta, \cos \theta/\cos(\theta - 2\delta)]. \quad (9)$$

Solving Eqs. (1), (2), and (6) together with the Bragg condition for the  $m$ th order

$$\lambda_B = 2d_{Bragg} \cos(\theta - \delta)/m, \quad (10)$$

where  $d_{Bragg}$  is the Bragg period, yields, to a first approximation, the following blaze condition for a multilayer-coated grating

$$md \sin \delta = nd_{Bragg}. \quad (11)$$

The numerous rigorous calculations performed by one of the present authors show Eqs. (7) and (9) to hold with a high accuracy at grazing incidence only for low-frequency gratings (300 grooves/mm and 600 gr/mm)<sup>3,4</sup>.

A fundamental constraint on the application of the above approach for bulk and multilayer soft-X-ray-EUV gratings, as well as for gratings with one dielectric coating, is imposed by the oblique angle of incidence, which should not be extremely grazing. For instance, the incidence angle for some bulk gratings should not exceed  $40^\circ$ <sup>11</sup>. The scalar efficiency obtained from Eq. (9) was found to differ from that calculated using the rigorous differential method<sup>11</sup> for a multilayer grating working at an incidence angle of  $45^\circ$ . The critical value of the angle depends, however, on the actual grating parameters and the wavelength and polarization. The incidence angle at which Eq. (9) still holds can in some cases be increased to  $70\text{--}80^\circ$ <sup>12</sup>. The limitation on the angle of incidence is connected with the difference in efficiency between the finitely and perfectly conductive bulk gratings operating in the soft-X-ray-EUV range under grazing incidence, particularly in the case of the TM polarization. The same applies to multilayer gratings if the radiation penetrates to some layer or down to the substrate. Numerous rigorous calculations based on the differential, integral, and modal methods, demonstrated a high accuracy that Eq. (7) provides in predicting the absolute maximum efficiency in the first and higher orders of a multilayer grating with an arbitrary groove profile (including a real profile, e.g., AFM-measured), which operates close to normal incidence. Obviously enough, the approach (7) can be valid only for highly conformal deposited layers, a condition met primarily in the soft-X-ray-EUV range. It was believed for a long time to be a very accurate and convenient method to calculate the absolute efficiency of multilayer, normal-incidence gratings operating in soft-X-ray-EUV wavebands.

### 3. EFFECT OF WAVELENGTH SEPARATION OF POSITIVE AND NEGATIVE GRATING ORDERS

As far as we know, noticeable separation in wavelength between the positive and negative orders in a multilayer grating operating close to normal incidence in the soft-X-ray–EUV range was first experimentally observed<sup>13</sup> in the first diffraction orders of a Mo/Si multilayer lamellar grating of 2400-gr/mm frequency operating at incidence angles of 10 and 32° (Fig. 1). The spectral separation of the +1 and –1 orders was attributed to the different angles of diffraction. This trend was confirmed in subsequent studies, including blaze gratings and higher orders<sup>5,14,15</sup>. The efficiency calculations performed in the above studies made use of a model based on Eq. (7) or its refined version (8), which takes into account the finite conductivity of the substrate and yields realistic results for both normal and grazing angles of incidence. While theoretical calculations based on the approximate physical models (7) and (8) predict quite well the peak shape and height of the efficiency curves in different orders, they do not yield, however, noticeable spectral separation of orders observed in experiments.

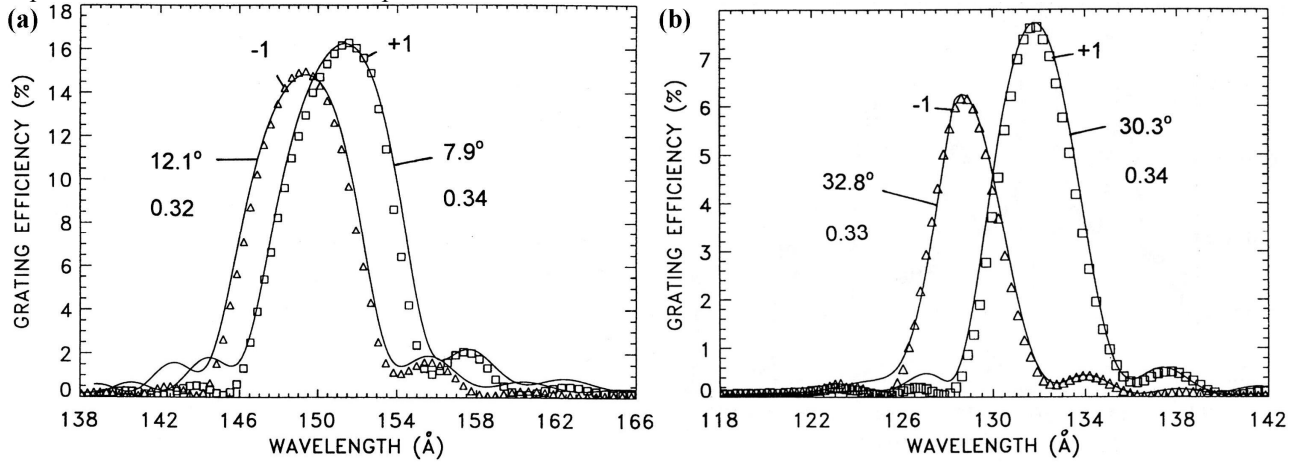


Fig. 1. Efficiencies in the +1 and –1 orders measured at an angle of incidence of 10° (a) and 32° (b) vs. wavelength. The solid curves are the reflectances of the multilayer coating for the indicated angles of incidence. The reflectance values were reduced by factors of 0.34 (a, b) and 0.32 (a) & 0.33 (b), which represent the groove efficiencies in the +1 and –1 orders, respectively.

The separation between positive and negative orders in wavelength for a grating with an arbitrary groove profile shape can be estimated from Eq. (5) for any order.

We find  $\theta'_n$  from the grating equation

$$\sin \theta - \sin \theta'_n = -n\lambda/d \quad (12)$$

taking into account the smallness of the angles of incidence and diffraction and substitute this expansion in Eq. (5)

$$D_n \approx 2\theta + n\lambda/d. \quad (13)$$

Next we write the difference  $\Delta\lambda_B$  between the spectral positions of the maxima in  $n$  and  $-n$  orders in the form

$$\Delta\lambda_B = \lambda_B(n) - \lambda_B(-n) = \lambda_{L,ii} [\cos (D_n/2) - \cos (D_{-n}/2)]. \quad (14)$$

After some manipulations made with due account of the smallness of the angles of incidence and diffraction we arrive at

$$\Delta\lambda_B \approx -\lambda_{L,ii} \lambda n \theta / d. \quad (15)$$

Equation (15) shows that the spectral separation of same plus and minus orders grows with increasing wavelength, angle of incidence, order number, and grating frequency. Strictly normal incidence does not give rise to order separation in wavelength.

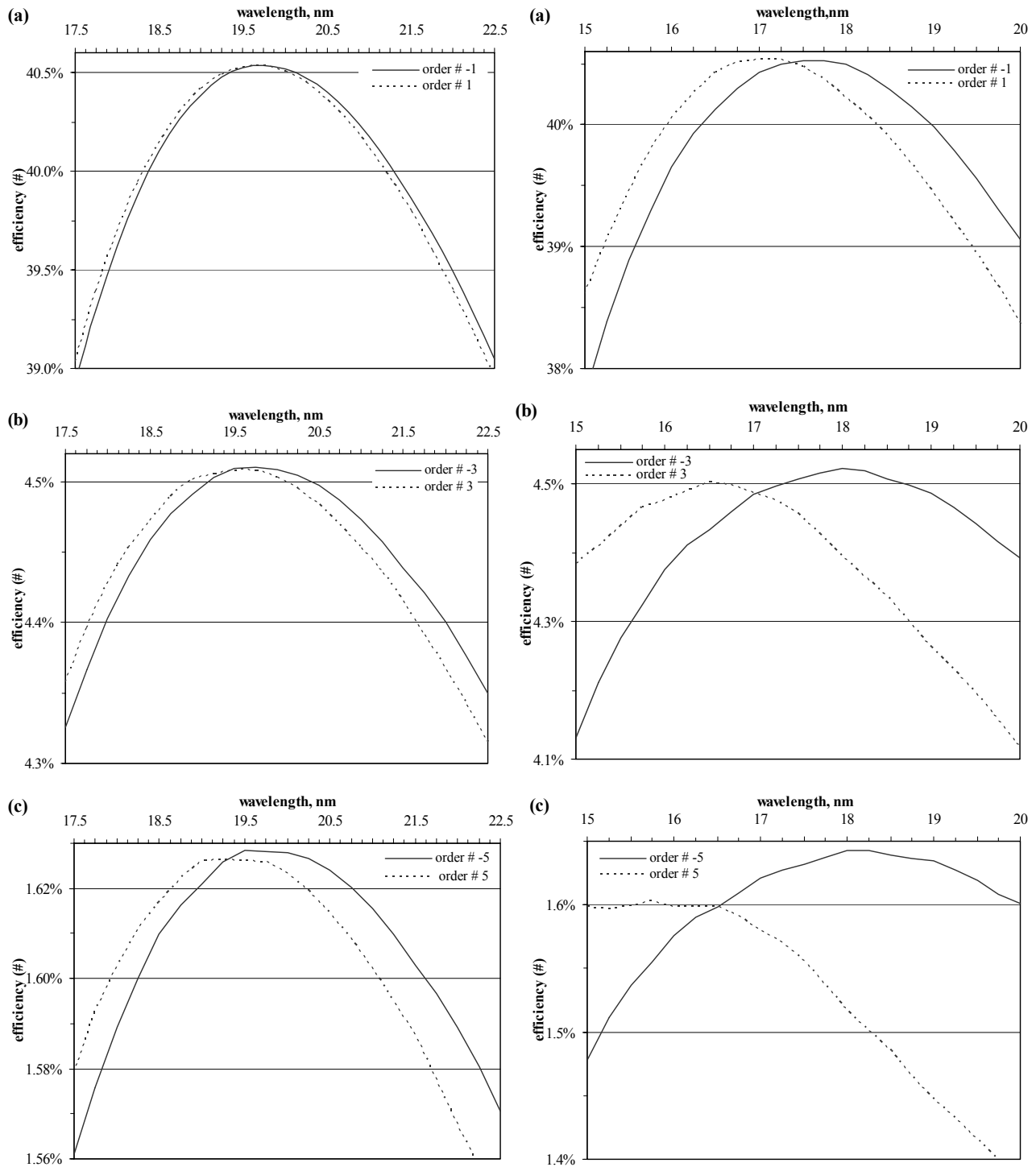


Fig. 2 (left column). Efficiency in the  $\pm 1$  (a),  $\pm 3$  (b), and  $\pm 5$  (c) orders rigorously calculated for a perfectly conductive 1200-gr/mm lamellar grating with 5-nm-deep grooves and 0.5 land-to-period ratio at an angle of incidence of  $10^\circ$  vs. wavelength.

Fig. 3 (right column). Efficiency in the  $\pm 1$  (a),  $\pm 3$  (b), and  $\pm 5$  (c) orders rigorously calculated for a perfectly conductive 1200-gr/mm lamellar grating with 5-nm-deep grooves and 0.5 land-to-period ratio at an angle of incidence of  $30^\circ$  vs. wavelength.

Compare now the values of  $\Delta\lambda_B$  obtained with the approximate relation (15) with the results of rigorous numerical modeling. As an illustration, consider gratings with perfect conductivity and a symmetric lamellar groove profile working in unpolarized radiation. Figures 2a,b,c display spectral response curves of efficiency in the  $\pm 1$ ,  $\pm 3$ ,  $\pm 5$  orders obtained for a 1200-gr/mm lamellar grating with 5-nm-deep grooves and 0.5 land-to-period ratio, with the maximum efficiency in the  $-1$  order lying in a wavelength of approximately 19.7 nm for an angle of incidence of  $10^\circ$ . Figures 3a,b,c present similar curves but for an angle of incidence of  $30^\circ$  and a corresponding peak efficiency at a wavelength of  $\sim 17.3$  nm. As seen from Figs. 2 and 3, the wavelength separation between efficiency maximums of positive and negative orders of the same number increases with increasing order number and angle of incidence, which is consistent with Eq. (15). The wavelength separation  $\Delta\lambda_B$  obtained from Eq. (15) for the first diffraction orders is  $0.8 \text{ \AA}$  for  $\theta = 10^\circ$ . As seen from Fig. 2, this value agrees well qualitatively with the separation between plus and minus orders derived in rigorous calculations for an angle of incidence of  $10^\circ$ . Another approximate value  $\Delta\lambda_B = 2.1 \text{ \AA}$  obtained using Eq. (15) for the angle of incidence of  $30^\circ$ , is about one half the actual separations between the corresponding plus and minus orders efficiency yielded in rigorous calculations (Fig. 3). This should be primarily attributed to the large angle of incidence, for which Eq. (15) is no longer accurate.

Figure 4 shows spectral response curves of efficiency in the  $\pm 1$ ,  $\pm 3$ ,  $\pm 5$  orders obtained for a 1200-gr/mm lamellar grating with 2.5-nm-deep grooves and 0.5 land-to-period ratio, which in the  $-1$  order peaks at a wavelength of approximately 8.7 nm for an angle of incidence of  $30^\circ$ . The separation in wavelength  $\Delta\lambda_B$  derived from Eq. (15) for the first diffraction orders is  $0.5 \text{ \AA}$ . As evident from Fig. 4, this value is in a quantitative agreement with the separations of positive and negative orders obtained for a  $30^\circ$  angle of incidence by rigorous calculations, despite the fairly large angle of incidence. This is accounted for by the small values of  $\lambda_{lit}$  and  $h_{opt}$  for which Eq. (15) is met with a high accuracy. A comparison of these curves in Fig. 4 with the corresponding graphs in Fig. 2 shows the spectral separation between the same plus and minus orders to grow approximately fourfold with the wavelength increasing by a factor two, which likewise is in good accord with Eq. (15).

Figure 5a,b,c presents spectral response curves of efficiency in  $\pm 1$ ,  $\pm 3$ , and  $\pm 5$  orders for a 2400-gr/mm lamellar grating with 5-nm-deep grooves, which for an angle of incidence of  $30^\circ$  peaks in  $-1$  order at a wavelength of approximately 17.3 nm. A comparison of the curves in Figs. 5 and 3 suggests that the wavelength separation of the efficiency maximums of orders is inversely proportional to grating period, a conclusion consistent with Eq. (15).

#### 4. INVESTIGATIONS OF SPECTRAL EFFICIENCY SEPARATION BETWEEN PLUS AND MINUS ORDERS OF MULTILAYER-COATED GRATINGS

The analysis outlined in Section 3 suggests a conclusion that the separation of positive and negative orders in wavelength is related to oblique, close-to-normal incidence of light on a grating operating in the short-wavelength spectral region and to different angles of deviation for these orders. The spectral separation of plus and minus orders equal in absolute magnitude is fitted well by the approximate relation (15) for small values of the parameter in parentheses on its right-hand side. This separation is, however, fairly small in absolute magnitude and, in view of the smoothly sloping efficiency curves of different orders obtained for bulk gratings, is of no particular significance for this type of grating. By contrast, for multilayer gratings whose efficiency maxima are determined by the Bragg reflection peaks separation between positive and negative orders in wavelength is reliably observable in various experiments<sup>5,7,13-16</sup> and significant.

To quantitatively study this effect as applied to multilayer gratings, one could modify Eqs. (7)–(9) to correct the angle of incidence  $\theta''$  in order to calculate the reflectance of a multilayer-coated mirror with due account of wavelength separation between positive and negative orders. One could, for instance, replace  $\theta''$  by the diffraction angle  $\theta'_n$  as this was done in<sup>13</sup> (Fig. 1a) or by the angle of deviation  $D_n$ , or again take the geometric mean of the reflectances of multilayer coatings calculated for the angles of incidence and diffraction<sup>17</sup>. Because of the approximate nature of this approach inherent in the physical model involved, it can yield a reasonable result in one case which would fit an experiment while proving erroneous in another<sup>12</sup>. Unfortunately, the exact outcome is not known in advance, and one should always perform a comparison with experiment or with rigorous calculations.

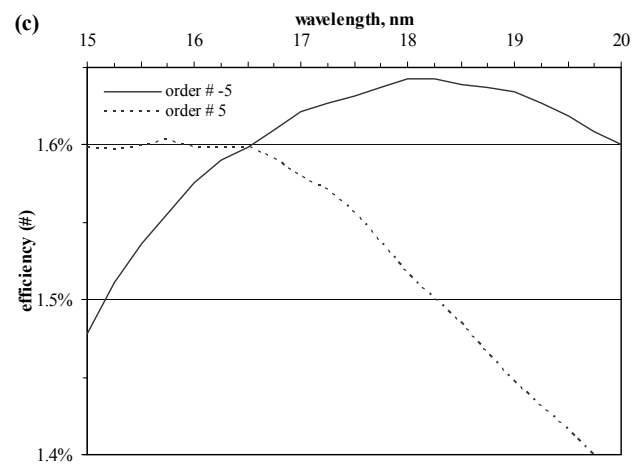
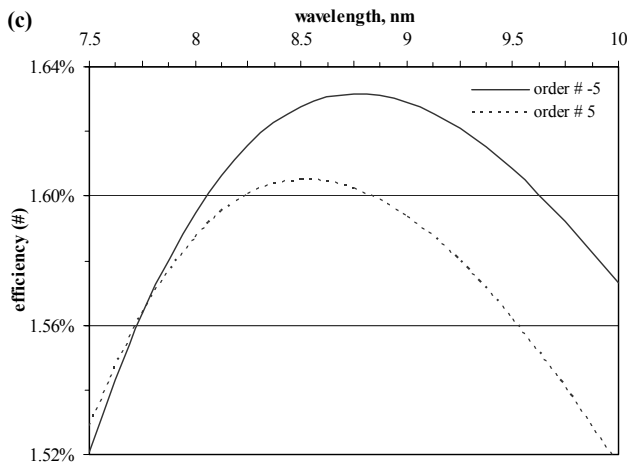
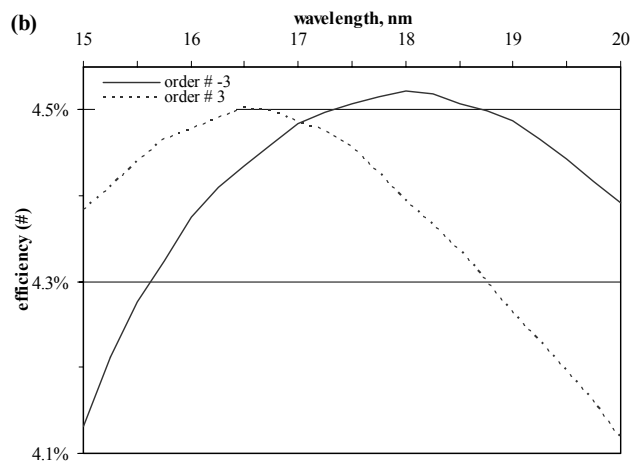
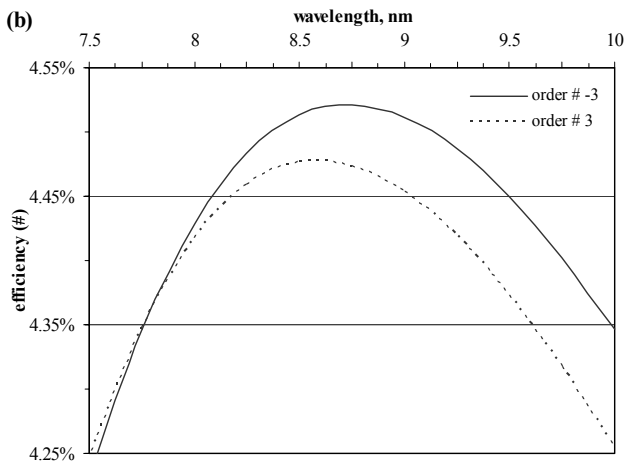
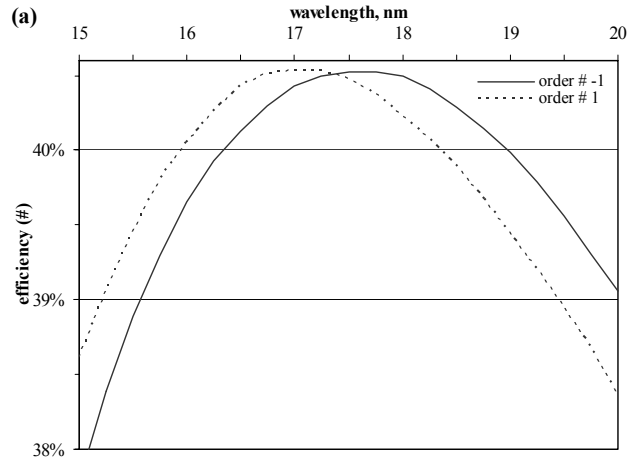
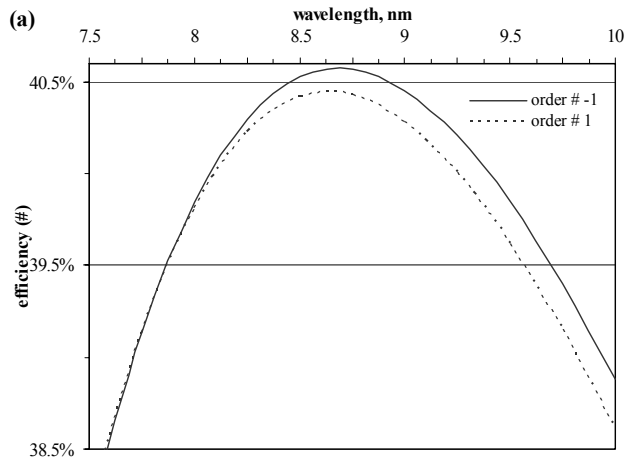


Fig. 4 (left column). Efficiency in the  $\pm 1$  (a),  $\pm 3$  (b), and  $\pm 5$  (c) orders rigorously calculated for a perfectly conductive 1200-gr/mm lamellar grating with 2.5-nm-deep grooves and 0.5 land-to-period ratio at an angle of incidence of  $30^\circ$  vs. wavelength.

Fig. 5 (right column). Efficiency in the  $\pm 1$  (a),  $\pm 3$  (b), and  $\pm 5$  (c) orders rigorously calculated for a perfectly conductive 2400-gr/mm lamellar grating with 5-nm-deep grooves and 0.5 land-to-period ratio at an angle of incidence of  $30^\circ$  vs. wavelength.

A numerical analysis of the experimentally observed spectral separation between positive and negative orders of multilayer gratings with a real groove profile was first carried out<sup>16</sup> by invoking the rigorous MIM method based on the multilayer scheme of boundary integral equations<sup>8</sup>. The calculations carried out<sup>16</sup> with the commercial code PCGrate-S(X) v.6.1<sup>9</sup> and modeling made with the use of the “resonance” mode (solver) permitted not only theoretical validation of the separation between positive and negative orders for a multilayer 2400-gr/mm Mo<sub>4</sub>Ru<sub>6</sub>/Be grating with a real, AFM-measured blaze groove profile but obtaining a good agreement with experiment, including high orders as well. This Section describes new efficiency calculations for a multilayer Mo/Si 4200-gr/mm grating with trapezoidal groove profile, which is designed for operation in the EIS spectrometer on the Solar-B spacecraft<sup>7</sup>.

The Solar-B mission scheduled for launch in 2006 is a joint collaboration<sup>18</sup> of the Space agencies of Japan, USA, and Great Britain developed within an International program of complex studies of the Sun, ILWS<sup>19</sup>. The spacecraft will be placed in a near-Earth polar solar-synchronous orbit of 600-km altitude and 97.9° inclination, where it would operate for several years. The EUV Imaging Spectrometer (EIS) designed for operation in the 17–21 and 25–29 nm wave bands is one of three Solar-B orbital instruments. The EIS is intended for recording high-resolution spectra of the solar corona and transition region integrated over short periods (3–10 s). The spectrometer pixel is 1.5 arc sec × 0.002 nm, the field of view is 400 arc sec, and the temperature range 1.e5–2.e7 K, which should provide resolution of Doppler-broadened lines at velocities of about 2 km/s and of nonthermal turbulent flows, of about 20 km/s. The shape of the spectral lines, their intensity and shift should provide determination of the velocity of solar vortices and of other plasma parameters, which should make possible relating corona dynamics observed with an X-ray telescope with the lower-lying photospheric magnetic field studied with an optical telescope. EIS is hoped to detect magnetic reconnection points and, by combining information gained by the two other telescopes, to settle the long-standing debates on the corona heating mechanisms and dynamics<sup>20</sup>.

Due to the high reliability and strength of multilayer Mo/Si coatings, they enjoy wide use in telescopes and normal-incidence spectrometers, both ground-based and spaceborne. The EIS developed for the Solar-B spacecraft is the first orbital instrument making use of a multilayer diffraction grating (DG), and the Mo/Si coating was chosen and optimized for its optics. The parabolic collecting mirror has a diameter of 160 mm and a focal length of 1.939 m. The toroidal DG, 100 mm in diameter and with a nominal radius of 1.18 m, having 4200 gr/mm and rectangular (trapezoidal) groove profile of nominal depth 58 Å, was fabricated holographically by Carl Zeiss, with subsequent ion etching of the fused silica substrate. The two halves of the mirror and of the DG were capped by a Mo/Si coating optimized for operation in two narrow EUV wave bands, which contain many emission spectral lines, including those of the He II, Fe XII, and Fe XXIV ions.

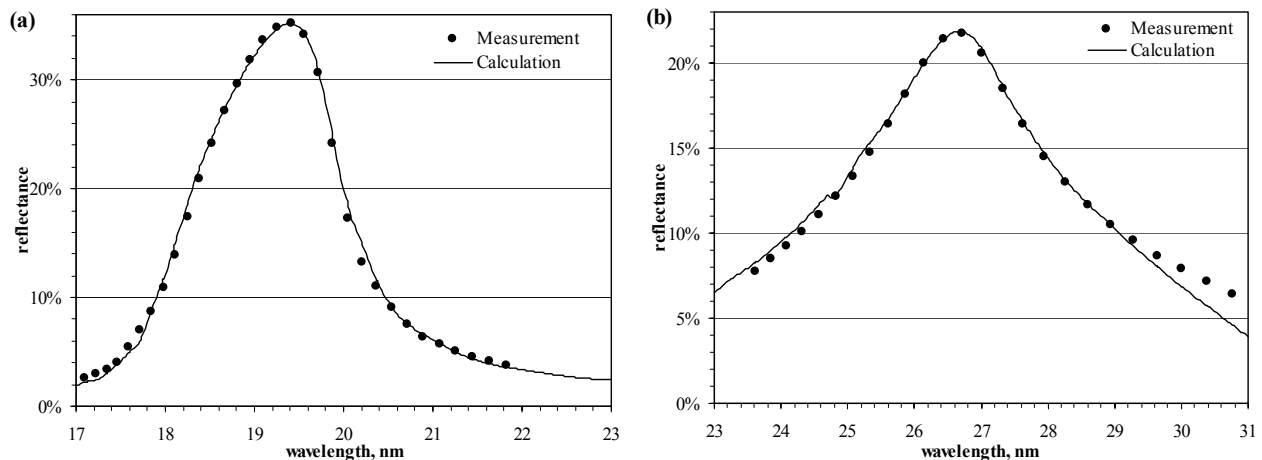


Fig. 6. The measured (data points) and the calculated (curves) reflectances of the short-band (a) and long-band (b) sides of the EIS mirror M2 vs. wavelength.

The multilayer coatings were applied to the test plane and full-sized concave mirrors and two pairs of flight optics at the Columbia Astrophysics Laboratory. The reflectances of the flight mirror M2 are displayed in Fig. 6. Points are

measurement data obtained with the synchrotron beam striking at an angle of incidence of  $2.15^\circ$  the mirror center between its short- and long-wavelength parts. The reflectances calculated with the use of refractive indices taken from different sources<sup>16</sup> are shown by lines. The reflectances and transmittances were calculated for each interface with the Debye–Waller factors accounting for their interdiffuseness nature and microroughness. The layer thicknesses and interface parameters were derived from X-ray measurements of plane mirror reflection made under grazing incidence. Small corrections were introduced into the sample periods and interface parameters to fit the calculated reflectance curves to measurements performed under normal incidence. The measurements of the multilayer FL1 grating were performed at the Naval Research Laboratory beamline X24C at the National Synchrotron Light Source at Brookhaven National Laboratory.

The efficiency was measured at 60 points of a square grid covering both parts of the working DG surface 90 mm in diameter. The X24C beamline<sup>21</sup> has a monochromator directing dispersed EUV radiation into the measurement chambers. The positions of the sample and the detector in the chamber are computer controlled. The efficiencies of the multilayer DG were measured at nine wavelengths with the radiation incident at an angle of  $6.5^\circ$  on the short-band side (from 17.1 to 22.0 nm) and at five wavelengths on the long-band side (from 25.1 to 29.3 nm) of the grating. To facilitate separation of the incident from diffracted beams, the angle of incidence was chosen slightly larger than the central angle of incidence on the DG in EIS ( $4.48^\circ$ ). Small changes of the angle of incidence near the normal affect, however, only weakly the DG efficiency variation<sup>7</sup>. Except for several extreme points at the edges of the working aperture, the efficiency was found to be quite uniform over the DG surface. The efficiencies of the FL1 grating measured at central points of its short- and long-wavelength sides (gravitation centers) are identified by markers in Fig. 7.

Theoretical DG efficiency was determined for unpolarized incidence radiation and parameters of the multilayer stack identical with the M2 mirror. For the short-band half of the DG, these parameters are: 20 Mo/Si layer pairs with a period of 10.3 nm and a Mo thickness to period ratio of 0.37; the Si-Mo interface rms is 0.2 nm, and the Mo-Si rms, 0.85 nm. For the long-band side, these parameters are 20, 14.35 nm, 0.34, 0.2 nm, and 0.85 nm, respectively. The Si protective cap layer is 2 nm thick. The trapezoidal groove profile based on AFM measurements is 6 nm deep, slopes of  $35^\circ$ , and equal top and groove widths<sup>7</sup>. The boundary profile was assumed the same for all layers.

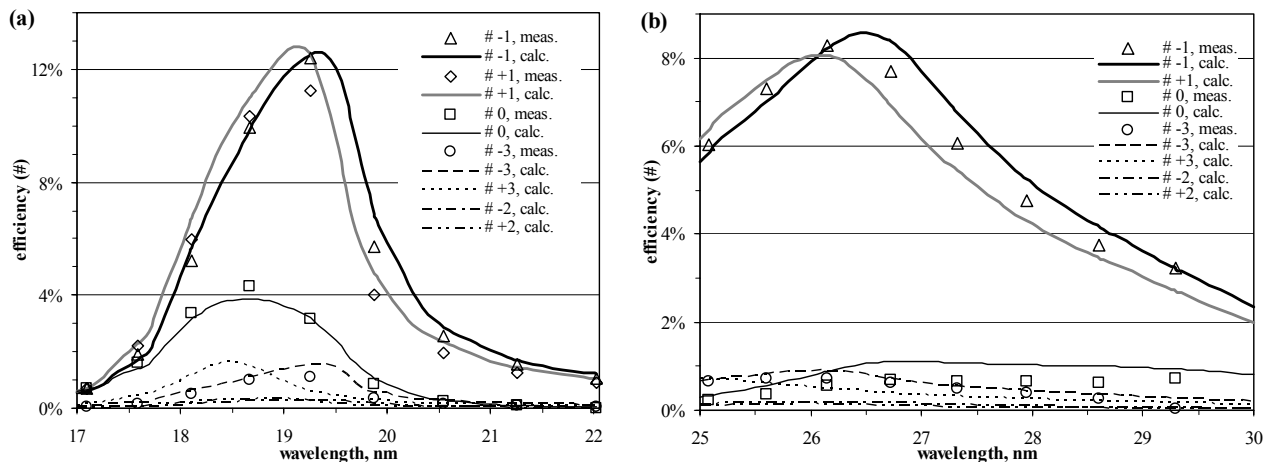


Fig. 7. The measured (data points) and the calculated efficiencies (curves) in orders of the short-band (a) and long-band (b) sides of the EIS grating FL1 vs. wavelength.

Figure 7 evidences good agreement between the measured and calculated diffraction efficiencies of the FL1 grating in  $-1$  and  $-3$  orders for both coatings. The agreement in the  $+1$  and  $0$  orders is somewhat worse, which can be ascribed to deviations in the groove profile and refractive indices used in the model<sup>16</sup>. The theoretical and experimental efficiencies of the FL1 grating, just as of another flight grating FL7, which were calculated with the approximate model (7) (at the “normal” calculation mode<sup>8,9</sup>), are presented in<sup>7,16</sup>. As pointed out above, the physical model based on Eq. (7) does not yield wavelength separation of the positive and negative orders and is not capable of accurately predicting the shape of the efficiency curves while determining well enough the height of their maxima. The time required to calculate one point for the FL1 grating efficiency (with the energy balance criteria  $\sim 0.01\%$ ) was about one second for the “normal”

calculation mode and about one minute for the “resonance” mode using an IBM® Think Pad with Intel® Pentium® M 1700 MHz processor, 1 MB Cache, 400 MHz Bus Clock, 512 MB RAM, and controlled by OS Windows® XP Pro.

## 5. CONCLUSION

Spectral separation of the positive and negative orders, which is observed experimentally, accounted for phenomenologically, and supported by rigorous numerical modeling, is associated with oblique incidence of radiation on a multilayer grating. It is observed with uncoated diffraction gratings too, while not very clearly pronounced<sup>7</sup>. For multilayer gratings operating in orders near the Bragg resonances, such separation of the same plus and minus orders in wavelength, although small, just as in the case of bulk gratings, is nevertheless quite substantial and, hence, should be taken into account in instrument manufacture and efficiency studies. This is a common property inherent in all multilayer diffraction gratings working in the soft-X-ray–EUV region under near-normal oblique incidence. As follows from both the approximate and rigorous approaches, it is the larger the longer the wavelength, the larger the angle of incidence, and the higher the groove frequency and diffraction order. To determine the spectral separation of the same positive and negative orders and the exact shape and position of efficiency curves, including gratings with real groove profiles, one should use codes based on rigorous electromagnetic theory for multilayer gratings, for instance, on the MIM method<sup>9</sup>.

## REFERENCES

1. R. Petit, ed., *Electromagnetic Theory of Gratings*, Springer, Berlin, 1980, Chap. 6.3.
2. L.M. Brekhovskih, *Waves in Layered Media*, Academic, New York, 1980, 2<sup>nd</sup> ed., 503 p.
3. L.I. Goray, “Numerical analysis of the efficiency of multilayer-coated gratings using integral method,” *Nucl. Inst. and Meth. A* **536**, pp. 211–221, 2005.
4. L.I. Goray, “Rigorous efficiency calculations for blazed gratings working in in- and off-plane mountings in the 5–50-Å wavelengths range,” *Proc. SPIE* **5168**, in *Optics for EUV, X-Ray, and Gamma-Ray Astronomy*, O. Citterio and S.L. O’Dell, eds., pp. 260–270, 2003.
5. L.I. Goray and J.F. Seely, “Efficiencies of master, replica, and multilayer gratings for the soft x-ray–EUV range: modeling based on the modified integral method and comparisons to measurements,” *Appl. Opt.* **41**, pp. 1434–1445, 2002.
6. H. Kierey, K. Heidemann, B. Kleemann, R. Winters, W. Egle, W. Singer, F. Melzer, R. Wevers and M. Antoni, EUV spectral purity filter: optical and mechanical design, gratings fabrication, and testing,” *Proc. SPIE* **5193**, in *Advances in Mirror Technology for X-Ray, EUV Lithography, Laser, and Other Applications*, A.M. Khounsary, U. Dinger, and K. Ota, eds., pp. 70–78, 2004.
7. J.F. Seely, Charles M. Brown, David L. Windt, Soizik Donguy, and Benjawan Kjornrattanawanich, “Normal-incidence efficiencies of multilayer-coated laminar gratings for the Extreme-Ultraviolet Imaging Spectrometer on the Solar-B mission,” *Appl. Opt.* **43**, pp. 1463–1471, 2004.
8. L.I. Goray and S.Yu. Sadov, “Numerical modelling of coated gratings in sensitive cases,” in *Trends in Optics and Photonics Series (TOPS 2002)*, OSA Diffractive Optics & Micro-Optics **75**, pp. 365–379, 2002.
9. Website at: <http://www.pcgrate.com>.
10. E.G. Loewen, M. Neviere, and D. Maystre, “On an asymptotic theory of diffraction gratings used in the scalar domain,” *JOSA* **68**, pp. 496–502, 1978.
11. B. Vidal, P. Vincent, P. Dhez, and M. Neviere, “Thin films and gratings: theories used to optimize the high reflectivity of mirrors and gratings for X-Ray optics,” *Proc. SPIE* **563**, in *Applications of Thin-Film Multilayered Structures to Figured X-Ray Optics*, pp. 142–149, 1985.
12. M. Neviere, “Multilayer coated gratings for x-ray diffraction: differential theory,” *JOSA A* **8**, pp. 1468–1473, 1991.
13. J.F. Seely, M.P. Kowalski, R.G. Cruddace, K.F. Heidemann, U. Heizmann, U. Kleineberg, K. Osterried, D. Menke, J.C. Rife, and W.R. Hunter, “Multilayer-coated laminar grating with 16% normal-incidence efficiency in the 150-Å wavelength region,” *Appl. Opt.* **36**, pp. 8206–8213, 1997.
14. J.F. Seely, “Review of multilayer normal-incidence gratings operating at 9 nm–40 nm wavelengths,” in *X-Ray Mirrors, Crystals, and Multilayers II*, A. Freund, A. Macrander, T. Ishikawa, and J. Wood, eds., *Proc. SPIE* **4782**, pp. 224–229, 2002.

15. B. Sae-Lao, S. Bajt, C. Montcalm, and J.F. Seely, "Performance of normal-incidence molybdenum–yttrium multilayer-coated diffraction grating at a wavelength of 9 nm," *Appl. Opt.* **41**, pp. 2394–2400, 2002.
16. J.F. Seely, L.I. Goray, D.L. Windt, Yu.A. Uspenskii, A.V. Vinogradov, B. Kjornrattanawanich, "Extreme ultraviolet optical constants for the design and fabrication of multilayer gratings," in *Optical Constants of Materials for UV to X-Ray Wavelengths*, R. Soufli and J.F. Seely, eds., *SPIE Proc.* **5538**, pp. 43–52, 2004.
17. M.C. Hutley, *Diffraction Gratings*, Academic, London, 1982, 330 p.
18. Website at: <http://www.isas.ac.jp/e/enterp/missions/solar-b/> .
19. Website at: <http://ilws.gsfc.nasa.gov/> .
20. S.V. Kuzin, I.A. Zhitnik, A.A. Pertsov, V.A. Slemzin, A.V. Mitrofanov, A.P. Ignatiev, V.V. Korneev, V.V. Krutov, I.I. Sobelman, E.N. Ragozin, R.J. Thomas, "Grazing Incidence XUV Spectroheliograph RES-C for the CORONAS-I Mission," *J. X-Ray Sci. and Technol.* **7**, pp. 233–247, 1997.
21. Website at: <http://spectroscopy.nrl.navy.mil/Synchro.html> .